Epileptic Activity Increases Cerebral Amino Acid Transport Assessed by ^{18}F-Fluoroethyl-L-Tyrosine Amino Acid PET: A Potential Brain Tumor Mimic

Markus Hutterer[1–3], Yvonne Ebner[3], Markus J. Riemenschneider[2,4], Antje Willuweit[5], Mark McCoy[6], Barbara Egger[7], Michael Schröder[1], Christina Wendl[8], Dirk Hellwig[9], Jirka Grosse[9], Karin Menhart[9], Martin Proescholdt[2,10], Brita Fritsch[11], Horst Urbach[12], Guenther Stockhammer[13], Ulrich Roelcke[14], Norbert Galldiks[5,15], Philipp T. Meyer[16], Karl-Josef Langen[5,17], Peter Hau[1,2], and Eugen Trinka[3]

[1]Department of Neurology, University of Regensburg Medical School, Regensburg, Germany; [2]Wilhelm Sander-Neurooncology Unit, University of Regensburg Medical School, Regensburg, Germany; [3]Department of Neurology and Centre for Cognitive Neuroscience, Christian-Doppler Klinik, Paracelsus Medical University Salzburg, Salzburg, Austria; [4]Department of Neuropathology, University of Regensburg Medical School, Regensburg, Germany; [5]Institute of Neuroscience and Medicine, Forschungszentrum Jülich, Jülich, Germany; [6]Department of Radiology and Division of Neuroradiology, Christian-Doppler Klinik, Paracelsus Medical University Salzburg, Salzburg, Austria; [7]Department of Nuclear Medicine, Landeskrankenhaus Salzburg, Paracelsus Medical University Salzburg, Salzburg, Austria; [8]Department of Radiology and Division of Neuroradiology, University of Regensburg Medical School, Regensburg, Germany; [9]Department of Nuclear Medicine, University of Regensburg Medical School, Regensburg, Germany; [10]Department of Neurosurgery, University of Regensburg Medical School, Regensburg, Germany; [11]Department of Neurology, University Hospital Freiburg, Freiburg, Germany; [12]Department of Neuroradiology, University Hospital Freiburg, Freiburg, Germany; [13]Department of Neurology, Medical University Innsbruck, Innsbruck, Austria; [14]Department of Neurology and Brain Tumor Center, Cantonal Hospital Aarau, Aarau, Switzerland; [15]Department of Neurology, University of Cologne, Cologne, Germany; [16]Department of Nuclear Medicine, University Hospital Freiburg, Freiburg, Germany; and [17]Department of Nuclear Medicine, University of Aachen, Aachen, Germany

O-(2-^{18}F-fluoroethyl)-L-tyrosine (^{18}F-FET) PET is a well-established method increasingly used for diagnosis, treatment planning, and monitoring in gliomas. Epileptic activity, frequently occurring in glioma patients, can influence MRI findings. Whether seizures also affect ^{18}F-FET PET imaging is currently unknown. The aim of this retrospective analysis was to investigate the brain amino acid metabolism during epileptic seizures by ^{18}F-FET PET and to elucidate the pathophysiologic background. **Methods:** Ten patients with 11 episodes of serial seizures or status epilepticus, who underwent MRI and ^{18}F-FET PET, were studied. The main diagnosis was glioma World Health Organization grade II–IV (n = 8); 2 patients suffered from nonneoplastic diseases. Immunohistochemical assessment of LAT1/LAT2/CD98 amino acid transporters was performed in seizure-affected cortex (n = 2) and compared with glioma tissues (n = 3). **Results:** All patients exhibited increased seizure-associated strict gyral ^{18}F-FET uptake, which was reversible in follow-up studies or negative shortly before and without any histologic or clinical signs of tumor recurrence. ^{18}F-FET uptake corresponded to structural MRI changes, compatible with cortical vasogenic and cytotoxic edema, partial contrast enhancement, and hyperperfusion. Patients with prolonged postictal symptoms lasting up to 8 wk displayed intensive and widespread (≥ 1 lobe) cortical ^{18}F-FET uptake. LAT1/LAT2/CD98 was strongly expressed in neurons and endothelium of seizure-affected brains and less in reactive astrocytosis. **Conclusion:** Seizure activity, in particular status epilepticus, increases cerebral amino acid transport with a strict gyral ^{18}F-FET uptake pattern. Such periictal pseudoprogression represents a potential pitfall of ^{18}F-FET PET and may mimic brain tumor. Our data also indicate a seizure-induced upregulation of neuronal, endothelial, and less astroglial LAT1/LAT2/CD98 amino acid transporter expression.

Key Words: epileptic seizure; status epilepticus; ^{18}F-FET PET; glioma; LAT1/2 expression

J Nucl Med 2017; 58:129–137
DOI: 10.2967/jnumed.116.176610

PET with the amino acid tracer *O*-(2-^{18}F-fluoroethyl)-L-tyrosine (^{18}F-FET) is increasingly used as an adjunct to magnetic resonance tomography (MRI) for brain tumor diagnosis, treatment planning, and monitoring (*1,2*). ^{18}F-FET uptake is primarily mediated by the system L amino acid transporter subtypes LAT1 and LAT2 (*3,4*). These transporters are heterodimers consisting of a light (LAT1, LAT2) and a heavy chain (CD98) and function as obligatory stereospecific exchanger (antiporter) of neutral amino acids (*3,4*).

LAT1/LAT2 are highly expressed in primary brain tumors. The highest levels have been detected in glioma cells and tumor-associated endothelium (*5*). Consequently, ^{18}F-FET PET has a high specificity for gliomas mediated by a tracer uptake almost independent of blood–brain barrier (BBB) dysfunction. ^{18}F-FET uptake by nonneoplastic tissue is considered as a rare phenomenon

Received Apr. 7, 2016; revision accepted Jun. 29, 2016.
For correspondence or reprints contact: Markus Hutterer, Department of Neurology and Wilhelm-Sander NeuroOncology Unit, University of Regensburg Medical School, Franz Josef Strauß-Allee 11, D-93053 Regensburg, Germany.
E-mail: markus.hutterer@gmx.at
Published online Jul. 28, 2016.

TABLE 1
Patient Characteristics at Time of Seizure Diagnosis

Case	Center	Age (y)	Sex	Diagnosis	Tumor localization	Treatment	Disease status	Seizure disorder before
1 + 2*	F	64	F	AA (1989)	Right frontal	SU, RA, CT 1989	SD, no residual tumor	Yes (motor SPS, TCS)
3	R	66	F	O (1985)	Right frontal	SU, RA, PCV 1985	SD, no residual tumor	Yes (motor SPS)
4	S	44	M	A (1991)	Left frontotemporal	SU 1991, 1996, 1997	SD, no residual tumor	Yes (TCS)
				OA (1996)		RA/BCNU 1997		
				AOA (1997)				
5	R	54	M	A (2014)	Left frontoparietal	SU, TMZ 2014	PD of residual tumor	Yes (motor SPS)
6	S	68	F	O (2004)	Right frontal	SU 2004	SD, residual tumor	Yes (motor SPS, TCS)
				AO (2011)		SU, RA/TMZ 05/2011		
						CCNU 11/2011		
7	R	51	M	GBM (2013)	Right frontal	SU 2013	ID of GBM	Yes (CPS, TCS)
8	R	29	F	A (2012)	Right frontoparietal	SU 2012, TMZ 2012–2013	PD of residual tumor	Yes (motor/sensory SPS, TCS)
				sGBM (2015)		SU + RA/TMZ 2015		
9	R	45	M	AO (2012)	Right frontotemporal	SU, RA/TMZ 2012	SD, residual tumor	No
						PC 2014		
						BEV/CCNU 2014–2015		
10	R	76	F	Nonconvulsive SE caused by septic encephalopathy (6/2013)		Anticonvulsive treatment	No recovery	Yes (nonconvulsive SE 4/2013)
11	S	66	F	Embolic cerebral ischemia (2011)		Anticonvulsive treatment	Seizure-free after 1 d	No

*Patient presented with same clinical symptoms and EEG findings according to SE in 2011 and 2014. At both time points combined MRI and ^{18}F-FET PET imaging was available.

F = Freiburg, Germany; R = Regensburg, Germany; S = Salzburg, Austria; O = oligodendroglioma WHO II; A = astrocytoma WHO II; OA = oligoastrocytoma WHO II; AA = anaplastic astrocytoma WHO III; AOA = anaplastic oligoastrocytoma WHO III; AO = anaplastic oligodendroglioma WHO III; GBM = glioblastoma WHO IV (s, secondary); SU = surgery; RA = radiotherapy; TMZ = temozolomide; BCNU = carmustine; CCNU = lomustine; PC = procarbazine + CCNU; PCV = procarbazine + CCNU + vincristine; BEV = bevacizumab; SD = stable disease; PD = progressive disease; ID = initial diagnosis.

TABLE 2

Overview on Seizure Activity, EEG Findings, MRI, and ^{18}F-FET PET Imaging and Disease Course of Study Population

Findings	Cases 1 and 2		Case 3: serial CPS followed by nonconvulsive SE, prolonged PS	Case 4: TCS followed by prolonged PS	Case 10: serial CPS followed by nonconvulsive SE (septic encephalopathy)	Case 5: daily (5–10) motor SPS followed by focal motor SE	Case 6: repeated motor SPS, secondarily TCS followed by focal acoustic SE	Case 11: TCS with PH	Case 7: repeated CPS and 1 secondarily TCS	Case 8: daily (1–3) sensory SPS	Case 9: daily (1–2) CPS
	TR serial motor SPS and focal SE, prolonged PH (2011)**	TR serial motor SPS and focal SE, prolonged PH (2014)**									
EEG	SA	SA	SE	SA	SE	SE	ED, SA	ED, SA	ED, SA	NA	SA
MRI											
Hem[+]	R	R	R	L	L	L	R	R	R	R	R
Lobe[+]	P, T, O	P, T, O	F, P, T	F, P, T	P, T, O	F	F, P	F	F	F	F
T1wCE[†]	+	+	+	–	–	–	–	–	–	–	–
T2/FLAIR[†]	++	++	++	++	++	++	+	+	+	–	–
DWI/ADC[†]	++	++	++	++	++	++	++	++	+	–	–
PWI[†]	++	++	++	NA	NA	++	NA	NA	NA	NA	–
^{18}F-FET PET*											
LBR_{max}	4.18	4.02	4.42	3.95	2.47	2.63	1.83	1.81	1.78	1.75	1.69
LBR_{mean}	2.58	2.50	2.45	2.08	1.68	1.71	1.46	1.42	1.54	1.57	1.43
MLV	236	271	212	203	76	26	19	23	8	16	12
Uptake extension[‡]	+++	+++	+++	+++	+++	++	++	+	+	+	+
Epi-PET duration[§]	Sim	Sim	6 d	4 d	5 d	7 d	5 d	3 d	5 d	Sim	Sim
Disease course											
Biopsy/surgery[¶]	BI^{EPI}	–	SU^{EPI}	–	–	–	SU^{EPI}	–	SU^{TU}	SU^{TU}	–
Symptom duration[‖]	4 w	4 w	NA	8 w	NR	2 w	1 w	1 d	1 d	–	–
^{18}F-FET PET preinvestigation (-) and follow-up (+)	+9w	+12 w	NA	+11 d, +12 w	NA	NA	–4 w	NA	+8 w	–10 w	+10 w
^{18}F-FET reversibility	Yes	Yes	–	Yes	–	–	Yes	–	Yes	Yes	Yes
LBR_{max}	1.22	1.24		2.34, 1.16			1.18		1.20	1.23	1.19
LBR_{mean}	1.09	1.11		1.45, 1.07			1.09		1.07	1.10	1.12
MLV	0	0		83, 0			0		0	0	0

*Evaluation of structural and metabolic cortical changes in MRI and ^{18}F-FET PET; [+]Tumor localization ([L] left, [R] right and [F] frontal, [P] parietal, [T] temporal, [O] occipital); [†]Visual assessment of cortical MRI changes ([–] no, [+] weak, [++] strong); [‡]Visual assessment of cortical ^{18}F-FET uptake extension ([+] focal [1 lobe and ≤ 5 cm], [++] enlarged [1 lobe and > 5 cm], [+++] widespread [more than 1 lobe]); [§]Time period between seizure onset or last EEG finding and ^{18}F-FET PET in (d) days or simultaneous (sim); [¶]SU^{TU}, surgery due to tumor progression; SU^{EPI}/BI^{EPI}, surgery/biopsy due to false-positive tumor diagnosis in MRI/PET; [–]No surgery/biopsy; [‖]Time period between seizure onset and complete recovery or adequate seizure control ([d] days, [w] weeks); **Patient presented with identical clinical symptoms and EEG findings in 2011 and 2014 and was evaluated twice.

ED = epileptic discharges; Hem = hemisphere; LBR = lesion-to-brain ratio; MLV = metabolic lesion volume (mL); NA = not assessed or available; NR = not recovered; PH = postictal hemiparesis; PS = postictal symptoms; SA = slow activity; Sim = simultaneous; TR = treatment-resistant.

and has been reported for various inflammatory and vascular brain lesions (*1,6–10*).

Epileptic seizures are among the most common symptoms of primary brain tumors (*11*). Focal symptoms after seizures usually disappear within 36 h (*12–14*). Prolonged postictal deficits, however, are often similar to symptoms that arise from progressive tumor growth. On the other hand, an increase of seizure frequency may be an early sign of tumor progression (*11,15*). Therefore, the differentiation of purely seizure-related postictal symptoms from tumor progression is of paramount importance in the clinical management of brain tumor patients.

To complicate this matter, seizure activity, in particular status epilepticus (SE), may result in MRI changes difficult to differentiate from tumor progression (*16*). For ^{18}F-FET PET, it is still unknown whether and to which extent seizures influence cerebral amino acid metabolism and ^{18}F-FET tracer uptake. Therefore, we retrospectively studied patients with serial epileptic seizures or SE who underwent MRI and ^{18}F-FET PET imaging, with a particular focus on spatial distribution pattern and time course of ^{18}F-FET uptake, and elucidated the pathophysiologic background by histopathologic assessment of amino acid transporter expression in specific cell types involved in epileptogenesis.

MATERIALS AND METHODS

Study Design and Data Collection

We identified 8 patients with glioma World Health Organization (WHO) grade II–IV and 2 patients with nonneoplastic diseases from 3 neurooncology centers (Salzburg, Austria; Regensburg and Freiburg, Germany), who fulfilled the following inclusion criteria: presentation with typical clinical or electroencephalographic (EEG) signs of highly frequent seizures (several times per day, serial seizures) or SE and multimodal imaging work-up consisting of ^{18}F-FET PET and serial MRI scans.

According to the definitions of the International League Against Epilepsy types of epileptic seizures were classified as simple partial seizure (SPS), complex partial seizure (CPS), tonic-clonic seizure (TCS), and series of epileptic seizures (SES) (*17*). SE was defined as ≥5 min of convulsive seizures or ≥10 min of nonconvulsive seizures with impairment of consciousness confirmed by EEG criteria (*18–20*).

Clinical data, laboratory values, EEG, standard MRI, ^{18}F-FET PET, and histologic records of all patients were analyzed (Table 1). Besides MRI and ^{18}F-FET PET during the course of disease, MR perfusion-weighted imaging (PWI), ^{99m}Tc-hexa-methyl-propylen-aminooxim (^{99m}Tc-HMPAO) SPECT, and ^{18}F-FDG PET scans at the time of epileptic disorder were additionally evaluated if available.

The local ethics committee of the University of Regensburg approved this retrospective study (no. 14-101-0185), and the requirement to obtain informed consent was waived. The study was conducted according to the standards of the Declaration of Helsinki in its recent revised version of 2013.

Standard MR Imaging

Standard MR imaging was routinely performed at the local departments of neuroradiology. At the time of seizure disorder and afterward in the course of disease, all patients underwent MRI scans using 1.5-T or 3.0-T scanners with standard head coils before and after administration of a gadolinium-based contrast agent. The routine MRI protocol included T1-weighted sequences with and without contrast agent (T1w, T1wCE), T2 and FLAIR (fluid-attenuated inversion recovery) sequences, and MR diffusion-weighted imaging (DWI) with calculation of the apparent diffusion coefficient (ADC). In 5 patients, additional dynamic susceptibility contrast (DSC) PWI was available.

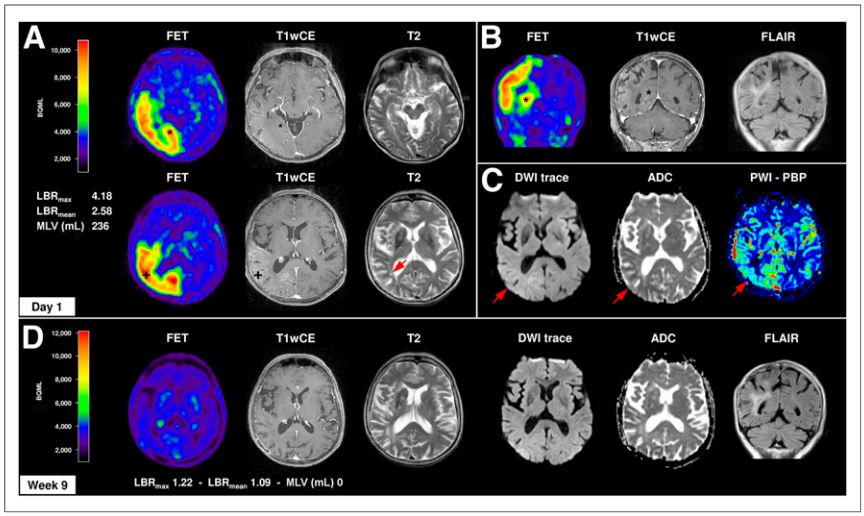

FIGURE 1. Structural and metabolic changes in MRI and ^{18}F-FET PET in focal SE. Case 1 represents a 64-y-old woman with clinically stable right frontal anaplastic astrocytoma WHO III without residual tumor. In 2011, she developed a series of treatment-refractory motor SPS and a focal SE of left arm and leg, followed by a severe and prolonged postictal left hemiparesis for 4 wk. (A–C) MRI/^{18}F-FET PET was performed simultaneously with motor SPS and revealed a distinct increased and extended cortical ^{18}F-FET uptake right temporo–parieto–occipital (LBR_{max}, 4.18; LBR_{mean}, 2.58) associated with cortical vasogenic (T2/FLAIR hyperintensity) and cytotoxic (diffusion-restriction in DWI + low ADC values) edema, contrast enhancement (T1wCE, BBB leakage), and hyperperfusion (PWI-PBP, baseline at peak map). ^{18}F-FET uptake was observed independently from BBB disruption in cortex with (*) and without (+) contrast enhancement in T1wCE. (D) Nine weeks after seizure onset and antiepileptic treatment, structural and metabolic MRI and ^{18}F-FET PET signal alterations completely resolved, except for slight cortical atrophy in T1 and T2/FLAIR. In 2014, same patient again developed treatment-resistant series of motoric SPS with prolonged postictal hemiparesis for 4 wk with similar morphologic and metabolic changes in MRI/^{18}F-FET PET (LBR_{max} 4.02, LBR_{mean} 2.50) (not shown).

MR Image Analysis

For study evaluation, the cortical changes in standard MRI and, if available, DSC-PWI were retrospectively reviewed by *2* independent investigators. During this analysis, contrast enhancement in T1wCE sequence (BBB permeability), T2/FLAIR sequences (hyperintensity, vascular edema), DWI/ADC sequences (diffusion restriction, cytotoxic edema), and DSC-PWI (hypo- or hyperperfusion) were graded visually on a 3-point scale (no, weak, and strong).

^{18}F-FET PET Imaging

^{18}F-FET PET was routinely performed at the local departments of nuclear medicine according to the German and Austrian guidelines for brain tumor imaging using labeled amino acid analogs (*21*). All patients fasted for at least 6 h before PET scanning. Before the investigation, a low-dose CT scan was obtained for attenuation correction. PET acquisition was started 20 min after intravenous injection of about 250 MBq of ^{18}F-FET

with a scan duration of at least 20 min. The methodologic differences between the different neurooncology centers (PET scanner equipment, reconstruction methods, and acquisition specifics) are summarized in Supplemental Table 1 (supplemental materials are available at http://jnm.snmjournals.org). All ^{18}F-FET PET scans were conducted between March 2011 and June 2015.

^{18}F-FET PET Image Analysis

^{18}F-FET PET and MR images were coregistered using dedicated software (Vinci V4.40; Max-Planck-Institute for Metabolism Research). The results were reviewed and, if necessary, adapted on the basis of anatomic landmarks. The region-of-interest (ROI) analysis was based on the summed static ^{18}F-FET PET data. The transaxial slice showing the highest tracer accumulation in the brain lesion was chosen for ROI analysis. The tracer uptake in the unaffected brain was determined by the largest possible ROI placed on the contralateral hemisphere in an area of normal-appearing brain, including white and gray matter and excluding basal ganglia, thalamus, and ventricles. ^{18}F-FET uptake was expressed as SUVs. The ROI of the suspicious lesion was determined using a 3-dimensional autocontouring process with a lesion-to-brain ratio (LBR) of $\geq$ 1.6 as described previously (*22*). Because of the reversibility of seizure-related cortical tracer uptake in follow-up studies and ^{18}F-FET PET shortly before seizure activity, cortical LBR_{max} was $<$ 1.6. In these cases, a circular ROI with a diameter of 1.6 cm was centered exactly on the cortex of maximal ^{18}F-FET uptake observed during seizure activity. Mean and maximum LBRs (LBR_{mean}, LBR_{max}) were calculated by dividing SUV_{mean} and SUV_{max} of the ^{18}F-FET uptake by the SUV_{mean} of the contralateral unaffected hemisphere.

For study evaluation, the cortical changes in ^{18}F-FET PET were assessed visually by 2 independent investigators. Cortical ^{18}F-FET uptake extension was graded as focal (extension $\leq$ 5 cm), enlarged (extension $>$ 5 cm, within 1 lobe), and widespread (more than 1 lobe).

In 1 patient (patient 3), a time–activity curve of SUV_{mean} in the frontal epileptic brain lesion was generated by measuring a spheric volume of interest of 2 mL centered on the maximal ^{18}F-FET brain lesion uptake and in a reference ROI of unaffected brain (as described above) using the entire dynamic dataset.

Histologic Assessment and Immunostaining

Histologic specimens were available for study analysis from 2 patients of the study cohort (Table 2): patient 3 with oligodendroglioma WHO grade II (no residual tumor) and nonconvulsive SE resulting in partial frontal lobe resection of seizure-affected cortex, and patient 7 with repeated CPS and TCS leading to first diagnosis of glioblastoma WHO grade IV and resection of seizure-affected cortex and subcortical tumor. Seizure-affected cortex was defined as cortical tissue with seizure-induced changes in MRI and ^{18}F-FET PET and without tumor cells in histopathologic evaluation.

For comparison, 3 tissue specimens of archival material with astrocytoma WHO grade II, anaplastic astrocytoma WHO grade III, and glioblastoma WHO grade IV were evaluated. All specimens were assessed for the protein expression pattern of LAT1, LAT2, and CD98 using formalin fixed and paraffin-embedded (FFPE) tissues.

Immunohistochemical staining was performed according to standard protocols. Paraffin sections were deparaffinized through an alcohol series and rehydrated. After antigen retrieval for 20 min (ethylene diamine tetraacetic acid buffer, pH 8.5; Sigma-Aldrich) and a blocking step, sections were incubated with the primary antibodies (LAT1/LAT2 for 45 min at room temperature, CD98 overnight at 4°C). The following primary antibodies were used: rabbit-anti SLC7A5 (PA2187 [Booster Immunoleader], 1:100), rabbit-anti SLC7A8 (NBP1-70389 [Novus Biologicals], 1:1,000), rabbit-anti CD98 (bs-6659R [Bioss], 1:100). Immunoreactivity was detected by the EnVision Detection System (#K406511-2; Dako) and 3,3′-diaminobenzidine tetrahydrochloride (EnVision+; Dako) and afterward counterstained by hematoxylin. As positive control, FFPE tissue from placenta was used, and negative controls were run without the primary antibody. Neuropathologic evaluation was performed by a board-certified neuropathologist masked to clinical and imaging findings. The immunostaining pattern of neurons, astrocytes, microglia, and tumor and vascular endothelial cells of tumor bulks and tumor infiltrative zones were analyzed separately.

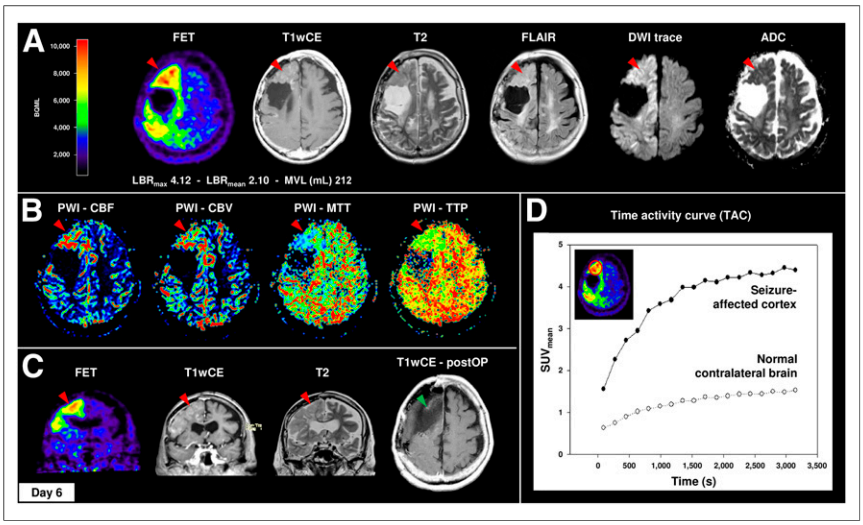

FIGURE 2. Widespread ^{18}F-FET uptake, vasogenic and cytotoxic edema, contrast enhancement, and hyperperfusion with strict gyral pattern during nonconvulsive SE. Case 3 demonstrates a 66-y-old woman with clinically stable right frontal oligodendroglioma WHO II without residual tumor. In 2014, the patient presented with repeated CPS followed by treatment-resistant nonconvulsive SE. ^{18}F-FET PET revealed distinct elevated cortical ^{18}F-FET uptake of right hemisphere with frontal and parietal accentuation (LBR_{max}, 4.42; LBR_{mean}, 2.45), corresponding to cortical contrast enhancement in T1wCE, marked gyral vasogenic (T2/FLAIR, cortical swelling), and cytotoxic (DWI/ADC) edema (A) and cortical hyperperfusion in DSC-PWI (B). (C) Clinical deterioration in combination with MRI and ^{18}F-FET PET imaging was interpreted as tumor recurrence. Therefore, patient underwent subtotal frontal lobe resection without any histologic evidence of tumor progression. (D) Additional ^{18}F-FET kinetic analysis of right frontal lesion and normal contralateral brain demonstrated SUV_{mean} time–activity course curve pattern with continuously increasing ^{18}F-FET uptake without washout. CBF = cerebral blood flow; CBV = cerebral blood volume; MTT = mean transit time; TTP = time to peak.

RESULTS

Study Population

In this multicenter study, 10 patients with 11 episodes of SES/SE were identified (8 patients with gliomas WHO grade II–IV; 2 patients with nonneoplastic diseases and final diagnoses of ischemic stroke and nonconvulsive SE caused by septic encephalopathy; Table 1). One patient presented with identical serial focal motor seizures and focal SE followed by prolonged postictal hemiparesis in 2011 and 2014. Because combined MRI and ^{18}F-FET PET was available from both time points, this patient was

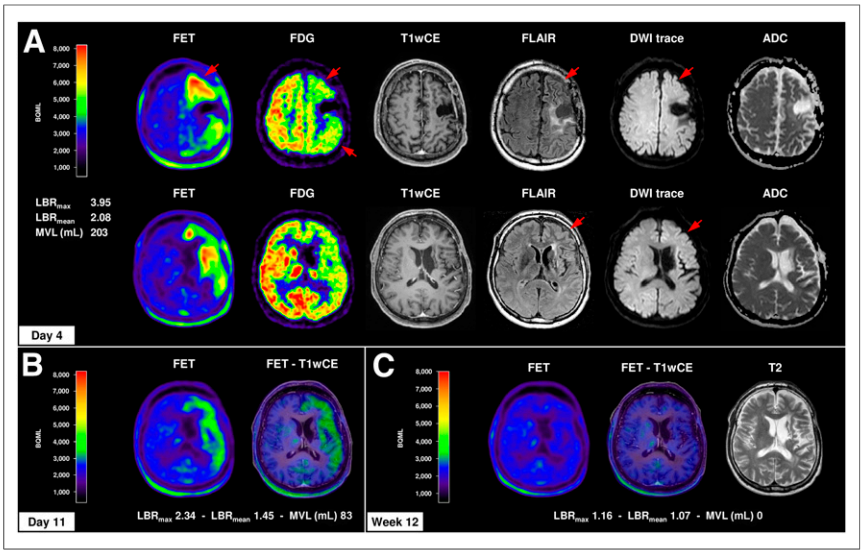

FIGURE 3. Cortical amino cid metabolism in ^{18}F-FET PET in course of prolonged postictal episode. Case 4 demonstrates 44-y-old man with clinically stable anaplastic astrocytoma WHO III without any residual tumor over years who presented with TCS followed by severe and prolonged postictal symptoms (global aphasia, right-sided hemiplegia, and hemineglect) over 8 wk. (A) MRI (day 1) and ^{18}F-FET PET (day 4) showed distinct increased and extended cortical ^{18}F-FET uptake of left brain hemisphere (LBR_{max}, 3.95; LBR_{mean}, 2.08) with frontal and temporal accentuation, corresponding to slight cortical vasogenic and cytotoxic edema (T2/FLAIR, DWI/ADC) without contrast enhancement (T1wCE). EEG monitoring, ^{18}F-FDG PET (glucose hypometabolism, red arrows), and ^{99m}Tc-HMPAO SPECT (hypoperfusion, only written medical report available), however, revealed no evidence of SE. (B) For ^{18}F-FET PET 11 d after symptom onset and 7 d after first ^{18}F-FET PET, slight regression of cortical ^{18}F-FET uptake (LBR_{max}, 2.34; LBR_{mean}, 1.45) was observed. (C) Patient slowly recovered within 8 wk after seizure onset. ^{18}F-FET PET and MRI 12 wk after symptom onset demonstrated complete recovery of cortical ^{18}F-FET uptake and brain edema; only residual cortical atrophy in T1 and T2/FLAIR sequences remained.

examined twice (cases 1 and 2). ^{18}F-FET PET was performed during or within 7 d after termination of the clinical or EEG signs of seizure activity (Table 2). MRI and ^{18}F-FET PET were also obtained out of an epileptic episode. This was during the clinical follow-up after seizure initiation in 5 cases (range, +8 to +12 wk) and before seizure onset in 2 other cases (−4 and −10 wk).

Structural MRI Changes During Seizure Activity

During SES/SE and prolonged postictal symptoms, we observed structural MRI changes including cortical hyperintensity in T2/FLAIR sequences and diffusion-restriction with low ADC values in DWI/ADC (9/11 cases; Table 2; Figs. 1–3; Supplemental Fig. 1), consistent with the presence of cortical vasogenic and cytotoxic edema. In 3 of 11 cases, additional focal gyral contrast enhancement in T1wCE was noted (Figs. 1 and 2). Cortical perfusion was increased in DSC-PWI in 3 of 5 available cases with clinical or electrophysiologic signs of SE or treatment-resistant series of SPS (Figs. 1–3). Patients with high seizure frequency but without SE (2/11 cases) did not exhibit any visible structural brain changes on standard MRI.

^{18}F-FET Uptake During Seizure Activity

Seven patients with SES/SE or prolonged postictal symptoms demonstrated increased ^{18}F-FET uptake strictly following the cortical ribbon of seizure-affected brain areas (patients 1–6 and 10; Table 2) corresponding to structural MRI changes. ^{18}F-FET PET revealed increased LBR_{max} (range, 1.83–4.42; median ± SD, 3.95 ± 1.02) and LBR_{mean} (range, 1.46–2.58; median ± SD, 2.27 ± 0.40). ^{18}F-FET tracer uptake occurred in areas with and without contrast enhancement in T1wCE (Figs. 1–3; Supplemental Figure 1). In contrast, patients with TCS followed by prolonged postictal hemiparesis (patient 11; Supplemental Fig. 1D) or high frequent seizures without SE (patients 7–9) exhibited lower LBR_{max} (range, 1.69–1.81; median ± SD, 1.77 ± 0.05) and LBR_{mean} (range, 1.42–1.57; median ± SD, 1.49 ± 0.08) of more focally enhanced cortical ^{18}F-FET uptake (Supplemental Fig. 1).

In case 3, the time–activity curve of ^{18}F-FET uptake in the frontal epileptic brain lesion was calculated and compared with the unaffected contralateral hemisphere (Fig. 2D). The curve pattern showed a continuously increasing ^{18}F-FET uptake without clear identifiable peak uptake and washout kinetics, comparable to that usually observed in low-grade gliomas.

^{18}F-FET Uptake and Prolonged Postictal Symptoms

Four SES/SE patients showed an increased and widespread cortical ^{18}F-FET uptake spreading into 2 or 3 lobes, combined with cortical vasogenic and cytotoxic edema and partial contrast enhancement in MRI (patients 1, 2, 5, and 6). This observation was associated with prolonged postictal symptoms lasting 1–6 wk (Table 2).

In contrast, patient 4 suffered from clinical stable anaplastic astrocytoma WHO grade III without residual tumor over years and presented with a TCS followed by severe postictal symptoms over 8 wk (Fig. 3). This condition was associated with distinctly increased cortical ^{18}F-FET uptake over 3 lobes of the left hemisphere with frontotemporal accentuation (LBR_{max}, 3.95; LBR_{mean}, 2.08) and slight cortical vascular and cytotoxic edema without contrast enhancement in MRI. Importantly, there was no evidence of SE in EEG monitoring, ^{18}F-FDG PET (regional hypometabolism), and ^{99m}Tc-HMPAO (regional hypoperfusion; not shown in detail), indicating prolonged increased cerebral amino acid metabolism in the postictal period.

Reversibility of Metabolic and Structural Cortical Changes

Follow-up MRI and ^{18}F-FET PET scans from 5 patients were available after seizure termination (range, 2–12 wk). Despite antiepileptic treatment, patients with widespread and extensive cortical ^{18}F-FET uptake showed only a slow recovery of structural and metabolic cortical changes within 4–12 wk (Table 2; Figs. 1D, 3B, and 3C). Figures 4A–4C show the time course of ^{18}F-FET uptake decrease. ^{18}F-FET PET scans were acquired 4 d (LBR_{max}, 3.95; LBR_{mean}, 2.08), 11 d (LBR_{max}, 2.34; LBR_{mean}, 1.45), and 12 wk (no tracer uptake) after seizure onset.

Histopathologic Evaluation and Immunostaining

Because MRI and ^{18}F-FET PET findings suggested tumor recurrence or progression, 3 patients underwent stereotactic biopsy

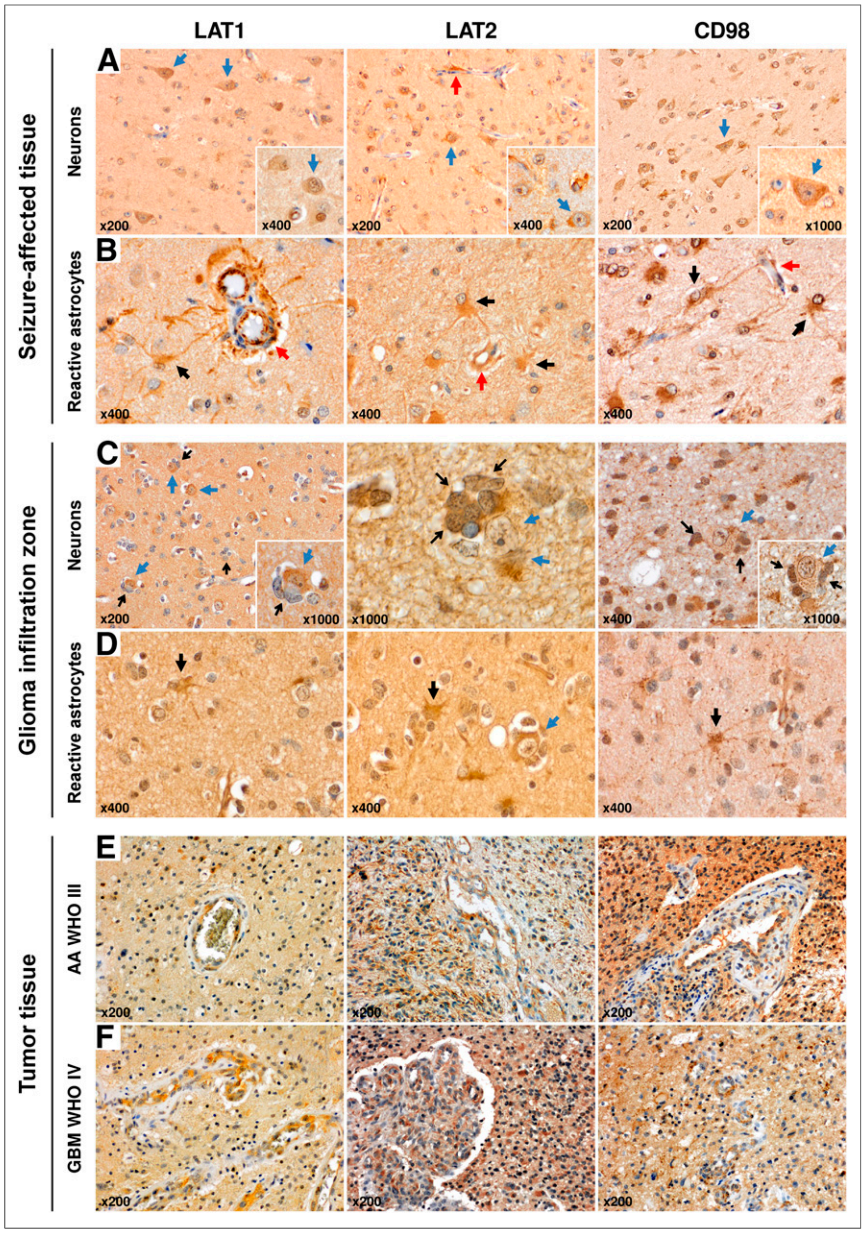

FIGURE 4. LAT1, LAT2, and CD98 protein expression pattern in seizure-affected and glioma tissue. (A) LAT1, LAT2, and CD98 showed strong and widespread expression in neurons of seizure-affected cortex obtained from patient with nonconvulsive SE and subtotal frontal lobe resection (case 3; Fig. 2; blue arrow, neuron; red arrow, vessel). (B) LAT1, LAT2, and CD98 were also detected in brain endothelial cells and reactive astrocytes (astrocyte–endothelium interaction as part of BBB; red arrow, vessel; black arrow, reactive astrocyte). Overall, LAT1, LAT2, and CD98 expression from neurons was more frequent than that from reactive astrocytes as reactive astrocytosis was only focally represented. (C) Within infiltration zone of astrocytoma WHO grade II cortical neurons revealed pronounced staining of LAT1/LAT2/CD98, in particular when glioma cells directly interact with neurons (tumor cells as satellites of neurons; blue arrow, neuron; open black arrow, satellitosis by tumor cells). (D) In addition, sporadic LAT1/LAT2/CD98-positive reactive astrocytes were observed within tumor infiltration zone. In comparison, tumor cells and tumor endothelium of anaplastic astrocytoma WHO grade III (E) and glioblastoma WHO grade IV (F) were also strongly positive for LAT1, LAT2, and CD98 expression.

or microsurgical resection of the putative lesions (patients 1, 3, and 6; Table 2). In those cases, standard neuropathologic evaluation of seizure-affected brain yielded cortical brain edema with reactive astrocytosis and microglial activation without any evidence of tumor cells.

On the basis of the known transport mechanisms of ^{18}F-FET, additional immunohistochemical analysis of LAT1, LAT2, and CD98 protein expression was performed using FFPE tissue specimens derived from partial frontal lobe resection of seizure-affected brain tissue in MRI and ^{18}F-FET PET (case 3; Figs. 2, 4A, and 4B) and tumor resection of a newly diagnosed glioblastoma WHO grade IV including histologic tumor-free cortex and subcortical tumor tissue (case 7). For comparison, 3 tissue samples from archival material with astrocytoma WHO grade II, anaplastic astrocytoma WHO grade III, and glioblastoma WHO grade IV were additionally evaluated (Figs. 4C–4F).

In seizure-affected cortex, LAT1/LAT2/CD98 amino acid transporter showed a strong and extended expression in neurons and brain endothelium (Figs. 4A and 4B) and was also detected in reactive astrocytes, especially when located adjacent to brain capillaries (Fig. 4B). Overall, LAT1/LAT2/CD98 staining in neurons and vascular endothelial cells was much more frequently observed than in reactive astrocytosis. Within the glioma infiltration zone, cortical neurons also revealed a pronounced expression of LAT1/LAT2/CD98, in particular when neurons and glioma cells interacted directly (tumor cells as satellites of neurons, Fig. 4C). Additionally, interspersed LAT1/LAT2/CD98-positive reactive astrocytes were observed (Fig. 4D). As expected, glioma and tumor-associated endothelial cells strongly expressed LAT1/LAT2/CD98 (Figs. 4E and 4F).

DISCUSSION

For the first time, we report a substantial increase of cortical amino acid transport assessed by ^{18}F-FET PET during and after serial seizures or SE in patients with gliomas and nonneoplastic brain lesions. Elevated ^{18}F-FET tracer uptake appears to be associated with cortical vasogenic and cytotoxic edema, hyperperfusion, and contrast enhancement in MRI. ^{18}F-FET uptake was clearly not caused by tumor progression or relapse in the subgroup of glioma patients, as proven by multimodal long-term follow-up MR/PET imaging and histologic confirmation in 3 patients. Therefore, our observation represents a so far unknown limitation of ^{18}F-FET PET in brain tumor diagnosis resembling periictal pseudoprogression.

^{18}F-FET uptake values in SES and SE patients were similar to those observed in high-grade gliomas (LBR_{max} median ± SD, SES and SE vs. high-grade gliomas, 3.95 ± 1.02 vs. 2.04 ± 0.72) (*1*).

In contrast, patients with frequent seizures but without SES and SE presented with lower and more focally pronounced cortical ^{18}F-FET uptake, comparable with values seen in low-grade gliomas (LBR_{max} median ± SD, seizures vs. low-grade gliomas, 1.77 ± 0.05 vs. 1.52 ± 0.70) (*1*). In addition, the time–activity curve pattern of ^{18}F-FET uptake corresponded to that described for low-grade gliomas (*23*). On the basis of these results, it appears that ^{18}F-FET tracer uptake values, and possibly dynamic ^{18}F-FET PET imaging, are not capable of distinguishing between seizure-induced alterations and tumor progression. In contrast, typical findings for seizure-induced ^{18}F-FET tracer uptake were the strict gyral uptake pattern and the reversibility in follow-up-studies. Although methodologic differences between the neurooncology centers exist (Supplemental Table 1), quantification of tracer uptake should in principle lead to similar results. In any case, it can be assumed that the methodologic differences are less relevant for intraindividual courses.

Structural changes of the brain cortex in MRI are the most stereotypic imaging features suggesting seizure activity or SE (*16*). On this account, the combination of a strict gyral, and mostly extended, ^{18}F-FET uptake associated with cortical MRI changes and high seizure activity, SE, or unusually prolonged postictal symptoms should raise the suspicion of periictal pseudoprogression. To avoid overtreatment, this phenomenon must be considered in the interpretation of ^{18}F-FET PET images and clinical decision making, especially in patients with cerebral glioma and symptomatic epilepsy.

In general, transient postictal deficits are reversible within 36 h (*12–14*). In our study population, however, prolonged postictal symptoms were observed for up to 8 wk after seizure termination and were associated with structural and metabolic cortical changes of more than 1 lobe in MRI and ^{18}F-FET PET. In all patients with follow-up investigations, increased gyral ^{18}F-FET uptake, cortical edema, contrast enhancement, and hyperperfusion normalized in parallel with clinical symptoms and EEG findings. Therefore, if clinically justified, a close clinical, MRI and ^{18}F-FET PET follow-up for at least 8 wk should be considered in these patients before therapeutic decisions, in particular invasive procedures, are undertaken.

Our findings also provide new insights into the pathophysiologic changes in seizure-associated cortical amino acid metabolism. Previous studies have shown that ^{18}F-FET does not participate in specific metabolic pathways and is transported predominantly via the system L amino acid transporters LAT1 and LAT2 (*3,4*). In normal cerebral cortex, LAT1 protein is only moderately expressed and LAT2 protein is absent (*24*). In contrast, immunohistochemical analysis of tissue specimens derived from seizure-affected cortex revealed a strong expression of LAT1/LAT2/CD98 in neurons and brain endothelium, indicating a seizure-induced upregulation of LAT1/LAT2 transporter mediating cortical ^{18}F-FET tracer uptake.

Interestingly, also neurons in the infiltration zone of glial tumors strongly expressed LAT1/LAT2/CD98, in particular when directly interacting with tumor cells as satellites (Fig. 4C). This observation supports the hypothesis of a link between LAT1/LAT2/CD98 expression and epileptogenesis, because in glial brain tumors epileptogenic activity arises in the cortex adjacent to the tumor, whereas the tumor itself is considered electrically inert with regard to seizure initiation (*25*). Structural and metabolic changes in the peritumoral tissue may lead to cortical cell alterations with imbalance between excitatory and inhibitory neurotransmitters, especially high intra- and peritumoral glutamate levels (*25–27*).

Reactive astrocytosis has been shown to be associated with increased ^{18}F-FET uptake in various nonneoplastic brain lesions (e.g., inflammatory and demyelinating lesions, brain ischemia and hemorrhage, brain abscesses, and radiation necrosis), representing another potential pitfall in ^{18}F-FET PET (*1,6–10*). In the presented group of patients, however, there were no clinical or radiologic signs that would have been consistent with 1 of these differential diagnoses. Furthermore, the presented lesions showed a strict gyral pattern, which is untypical for the lesions mentioned above and suggests a connection with an epileptogenic genesis. This notion is further supported by the fact that in specimens of seizure-affected cortex, LAT1/LAT2/CD98 was more strongly expressed in neurons and brain endothelium than in reactive astrocytes, indicating a predominant neuronal ^{18}F-FET uptake during seizure activity.

Other aspects that need to be discussed concern the relationship of seizure-mediated increased ^{18}F-FET uptake, regional blood flow, and BBB disruption. Numerous PET and SPECT studies using various tracers have shown that the cerebral blood flow is increased in the ictal and decreased in the interictal state (*28*). In the present report, enhanced cortical ^{18}F-FET uptake was observed in brain areas with increased (Figs. 1–3) and decreased regional perfusion as well as increased (Supplemental Fig. 1) and decreased (Fig. 3) glucose metabolism. Similarly, previous studies have shown high ^{18}F-FET uptake in gliomas with low cerebral blood flow or blood volume (*29,30*). Therefore, it is unlikely that increased ^{18}F-FET uptake during seizure activity is caused by hyperperfusion to a major extent.

Along with gyral hyperperfusion most SES/SE patients developed a mixture of vasogenic and cytotoxic edema, and partly contrast enhancement in MRI, indicating enhanced permeability or disruption of the BBB. BBB dysfunction is one of the earliest pathophysiologic features of SE mediated by several mechanisms, including glutamate receptor activation of endothelial cells, rapidly activated brain inflammation, and seizure-associated angiogenesis (*31,32*).

Although a correlation between ^{18}F-FET uptake and contrast enhancement in brain tumors has been reported (*1*), there are many examples of brain lesions with BBB disruption and contrast enhancement (e.g., radionecrosis, abscesses) that are clearly negative on ^{18}F-FET PET. This observation excludes that ^{18}F-FET uptake is significantly influenced by BBB disruption. Therefore, it is most likely that the observed phenomenon of increased ^{18}F-FET uptake in epileptogenic brain areas is due to a process that mediates an upregulation of LAT1/LAT2/CD98 expression in neurons and the brain endothelium.

Enhanced amino acid uptake during seizure activity has also been discussed in a few case reports using ^{11}C-methionine (*33–35*), which is also transported via LAT1/LAT2 (*36*). Moreover, increased amino acid uptake in epileptic foci was reported for PET using α-^{11}C-methyl-L-tryptophan (*37,38*), which measures the serotonin synthesis rate. It was speculated that its increased uptake in epileptogenic tubers reflects changes in the kynurenine pathway. Since L-tryptophan is also a substrate of LAT1/LAT2 (*39*), it is tempting to hypothesize that increased α-^{11}C-methyl-L-tryptophan uptake in epileptogenic foci has also been influenced by increased LAT1/LAT2 transport as observed in the present study for ^{18}F-FET.

CONCLUSION

Seizure-induced increase of cerebral amino acid transport seems to be primarily mediated by neuronal, endothelial, and to a

lesser extent astroglial LAT1/LAT2/CD98 expression. A strict gyral ^{18}F-FET uptake in combination with cortical MRI changes, high seizure activity, and unusually prolonged postictal focal symptoms should raise the suspicion of periictal pseudoprogression. To avoid overtreatment, this phenomenon has to be considered in the interpretation of ^{18}F-FET PET images, and a close clinical and MRI/^{18}F-FET PET reevaluation for at least 8 wk should be considered.

DISCLOSURE

No potential conflict of interest relevant to this article was reported.

ACKNOWLEDGMENTS

We thank Nicole Niemietz and Maria Hirblinger for excellent technical assistance. Parts of the study were presented at the 2014 Scientific Meeting of the Society for Neurooncology (SNO) as a poster.

REFERENCES

1. Hutterer M, Nowosielski M, Putzer D, et al. [^{18}F]-fluoro-ethyl-L-tyrosine PET: a valuable diagnostic tool in neuro-oncology, but not all that glitters is glioma. *Neuro-oncol.* 2013;15:341–351.
2. Galldiks N, Langen KJ, Pope WB. From the clinician's point of view: what is the status quo of positron emission tomography in patients with brain tumors? *Neuro-oncol.* 2015;17:1434–1444.
3. Langen KJ, Hamacher K, Weckesser M, et al. O-(2-[^{18}F]fluoroethyl)-L-tyrosine: uptake mechanisms and clinical applications. *Nucl Med Biol.* 2006;33:287–294.
4. Habermeier A, Graf J, Sandhofer BF, Boissel JP, Roesch F, Closs EI. System L amino acid transporter LAT1 accumulates O-(2-fluoroethyl)-L-tyrosine (FET). *Amino Acids.* 2015;47:335–344.
5. Haining Z, Kawai N, Miyake K, et al. Relation of LAT1/4F2hc expression with pathological grade, proliferation and angiogenesis in human gliomas. *BMC Clin Pathol.* 2012;12:4–12.
6. Spaeth N, Wyss MT, Weber B, et al. Uptake of ^{18}F-fluorocholine, ^{18}F-fluoroethyl-L-tyrosine, and ^{18}F-FDG in acute cerebral radiation injury in the rat: implications for separation of radiation necrosis from tumor recurrence. *J Nucl Med.* 2004;45:1931–1938.
7. Floeth FW, Pauleit D, Sabel M, et al. ^{18}F-FET PET differentiation of ring-enhancing brain lesions. *J Nucl Med.* 2006;47:776–782.
8. Salber D, Stoffels G, Pauleit D, et al. Differential uptake of [^{18}F]FET and [^{3}H]l-methionine in focal cortical ischemia. *Nucl Med Biol.* 2006;33:1029–1035.
9. Salber D, Stoffels G, Pauleit D, et al. Differential uptake of O-(2-^{18}F-fluoroethyl)-L-tyrosine, L-^{3}H-methionine, and ^{3}H-deoxyglucose in brain abscesses. *J Nucl Med.* 2007;48:2056–2062.
10. Salber D, Stoffels G, Oros-Peusquens AM, et al. Comparison of O-(2-^{18}F-fluoroethyl)-L-tyrosine and L-^{3}H-methionine uptake in cerebral hematomas. *J Nucl Med.* 2010;51:790–797.
11. van Breemen MS, Wilms EB, Vecht CJ. Epilepsy in patients with brain tumours: epidemiology, mechanisms, and management. *Lancet Neurol.* 2007;6:421–430.
12. Fagan KJ, Lee SI. Prolonged confusion following convulsions due to generalized nonconvulsive status epilepticus. *Neurology.* 1990;40:1689–1694.
13. Rolak LA, Rutecki P, Ashizawa T, Harati Y. Clinical features of Todd's post-epileptic paralysis. *J Neurol Neurosurg Psychiatry.* 1992;55:63–64.
14. Shorvon S, Trinka E. Nonconvulsive status epilepticus and the postictal state. *Epilepsy Behav.* 2010;19:172–175.
15. Vecht CJ, Kerkhof M, Duran-Pena A. Seizure prognosis in brain tumors: new insights and evidence-based management. *Oncologist.* 2014;19:751–759.
16. Rheims S, Ricard D, van den Bent M, et al. Peri-ictal pseudoprogression in patients with brain tumor. *Neuro-oncol.* 2011;13:775–782.
17. Fisher RS, van Emde Boas W, Blume W, et al. Epileptic seizures and epilepsy: definitions proposed by the International League Against Epilepsy (ILAE) and the International Bureau for Epilepsy (IBE). *Epilepsia.* 2005;46:470–472.
18. Trinka E, Cock H, Hesdorffer D, et al. A definition and classification of status epilepticus: report of the ILAE Task Force on Classification of Status Epilepticus. *Epilepsia.* 2015;56:1515–1523.
19. Beniczky S, Hirsch LJ, Kaplan PW, et al. Unified EEG terminology and criteria for nonconvulsive status epilepticus. *Epilepsia.* 2013;54(suppl 6):28–29.
20. Trinka E, Leitinger M. Which EEG patterns in coma are nonconvulsive status epilepticus? *Epilepsy Behav.* 2015;49:203–222.
21. Langen KJ, Bartenstein P, Boecker H, et al. German guidelines for brain tumour imaging by PET and SPECT using labelled amino acids. *Nuklearmedizin.* 2011;50:167–173.
22. Pauleit D, Floeth F, Hamacher K, et al. O-(2-[^{18}F]fluoroethyl)-L-tyrosine PET combined with MRI improves the diagnostic assessment of cerebral gliomas. *Brain.* 2005;128:678–687.
23. Galldiks N, Rapp M, Stoffels G, et al. Response assessment of bevacizumab in patients with recurrent malignant glioma using [^{18}F]fluoroethyl-L-tyrosine PET in comparison to MRI. *Eur J Nucl Med Mol Imaging.* 2013;40:22–33.
24. Uhlén M, Fagerberg L, Hallstrom BM, et al. Proteomics: tissue-based map of the human proteome. *Science.* 2015;347:1260419.
25. Wolf HK, Roos D, Blumcke I, Pietsch T, Wiestler OD. Perilesional neurochemical changes in focal epilepsies. *Acta Neuropathol (Berl).* 1996;91:376–384.
26. Marcus HJ, Carpenter KL, Price SJ, Hutchinson PJ. In vivo assessment of high-grade glioma biochemistry using microdialysis: a study of energy-related molecules, growth factors and cytokines. *J Neurooncol.* 2010;97:11–23.
27. Buckingham SC, Campbell SL, Haas BR, et al. Glutamate release by primary brain tumors induces epileptic activity. *Nat Med.* 2011;17:1269–1274.
28. Sarikaya I. PET studies in epilepsy. *Am J Nucl Med Mol Imaging.* 2015;5:416–430.
29. Wyss MT, Hofer S, Hefti M, et al. Spatial heterogeneity of low-grade gliomas at the capillary level: a PET study on tumor blood flow and amino acid uptake. *J Nucl Med.* 2007;48:1047–1052.
30. Filss CP, Galldiks N, Stoffels G, et al. Comparison of ^{18}F-FET PET and perfusion-weighted MR imaging: a PET/MR imaging hybrid study in patients with brain tumors. *J Nucl Med.* 2014;55:540–545.
31. Gorter JA, van Vliet EA, Aronica E. Status epilepticus, blood-brain barrier disruption, inflammation, and epileptogenesis. *Epilepsy Behav.* 2015;49:13–16.
32. Chen JW, Wasterlain CG. Status epilepticus: pathophysiology and management in adults. *Lancet Neurol.* 2006;5:246–256.
33. Madakasira PV, Simkins R, Narayanan T, Dunigan K, Poelstra RJ, Mantil J. Cortical dysplasia localized by [^{11}C]methionine positron emission tomography: case report. *AJNR.* 2002;23:844–846.
34. Lopci E, Bello L, Chiti A. ^{11}C-methionine uptake in secondary brain epilepsy. *Rev Esp Med Nucl Imagen Mol.* 2014;33:234–236.
35. Sasaki M, Kuwabara Y, Yoshida T, et al. Carbon-11-methionine PET in focal cortical dysplasia: a comparison with fluorine-18-FDG PET and technetium-99m-ECD SPECT. *J Nucl Med.* 1998;39:974–977.
36. Okubo S, Zhen HN, Kawai N, Nishiyama Y, Haba R, Tamiya T. Correlation of L-methyl-^{11}C-methionine (MET) uptake with L-type amino acid transporter 1 in human gliomas. *J Neurooncol.* 2010;99:217–225.
37. Chugani DC, Chugani HT, Muzik O, et al. Imaging epileptogenic tubers in children with tuberous sclerosis complex using alpha-[^{11}C]methyl-L-tryptophan positron emission tomography. *Ann Neurol.* 1998;44:858–866.
38. Juhász C, Chugani DC, Muzik O, et al. Alpha-methyl-L-tryptophan PET detects epileptogenic cortex in children with intractable epilepsy. *Neurology.* 2003;60:960–968.
39. Krämer SD, Mu L, Muller A, et al. 5-(2-^{18}F-fluoroethoxy)-L-tryptophan as a substrate of system L transport for tumor imaging by PET. *J Nucl Med.* 2012;53:434–442.